Eur. Phys. J. C manuscript No.
(will be inserted by the editor)

Wigner distributions and orbital angular momentum of a proton

D. Chakrabarti[1], T. Maji[1], C. Mondal[1] · A. Mukherjee[2]

arXiv:1601.03217v2 [hep-ph] 12 Jul 2016

Received: date / Revised version: date

Abstract The Wigner distributions for u and d quarks in a proton are calculated using the light front wave functions (LFWFs) of the scalar quark-diquark model for nucleon constructed from the soft-wall AdS/QCD correspondence. We present a detail study of the quark orbital angular momentum(OAM) and its correlation with quark spin and proton spin. The quark density distributions, considering the different polarizations of quarks and proton, in transverse momentum plane as well as in transverse impact parameter plane are presented for both u and d quarks.

1 Introduction

A complete understanding of partonic structure of nucleon is one of the challenging tasks in the particle physics. Both theoretical and experimental efforts are going on to unravel the three dimensional distributions of the partons and their contributions to the nucleon spin and angular momentum. Because of the nonperturbative nature of QCD, it is very difficult to perform first principle calculations of the hadron properties. However a perturbative approach in light cone framework allows us to calculate the parton distribution function(PDF), $f(x)$, which gives the probability of having a parton with light-cone longitudinal momentum fraction x inside a nucleon but it contains no information about the transverse structure or angular momentum distributions. The spin correlation of partons are described by the helicity distribution, $g_1(x)$, and transversity distributions, $h_1(x)$. The generalized parton distributions(GPDs) and the transverse momentum dependent distributions(TMDs) encode informations about the three dimensional structure of the nucleons. In the deeply virtual Compton scattering(DVCS), deeply virtual meson electroproduction (DVMPs), a more general views of parton distributions, in the collinear frame, is studied by GPDs[1,2,3,4] which are functions of longitudinal momentum and two transverse impact parameter coordinates. TMDs[5,6,7,8] are functions of the transverse momentum of the parton and appear in the semi inclusive deep inelastic scattering(SIDIS) where the collinear picture is no longer enough to explain the single spin asymmetry(SSA).

Wigner distributions are six dimensional distributions containing more general informations about the nucleon structure. Wigner distributions do not have probabilistic interpretation but in certain limits, reduce to GPDs and TMDs. The Wigner distributions are defined as functions of three momentums and three positions of a parton inside a nucleon. The concept of Wigner distributions was first introduced in [9]. In [10], five dimensional Wigner distributions were proposed in the light-front formalism with three momentum and two position components of a parton. Wigner distributions integrated over transverse momentum give the GPDs at zero skewness, the TMDs are obtained by integrating over transverse impact parameters with zero momentum transfer and the integration over transverse momentum and transverse positions provide the PDFs. The Wigner distributions after integrating over the light cone energy of the parton are interpreted as a Fourier transform of corresponding generalized transverse momentum dependent distributions (GTMDs) which are functions of the light cone three-momentum of the parton as well as the momentum transfer to the nucleon.

Department of Physics, Indian Institute of Technology Kanpur, Kanpur 208016, India
· Department of Physics, Indian Institute of Technology Bombay, Mumbai 400076, India

Angular momentum of a quark is extracted from Wigner distributions taking the phase space average. The spin-spin and spin-orbital angular momentum(OAM) correlations between a nucleon and a quark inside the nucleon can also be described from phase space average of Wigner distributions. Wigner distributions have been studied in different models e.g., in lightcone constituent quark model[11,12], in chiral soliton model[13, 14], light front dressed quark model[15], lightcone spectator model[16]. In this work, we investigate the Wigner distributions for unpolarized and polarized proton and the orbital angular momentum(OAM) and spin-spin and spin-OAM correlations in a scalar diquark model of proton [17] with the light front wavefunctions modeled from AdS/QCD prediction.

The paper is organized as follows. We first introduce the lightfront scalar diquark model in Sec.2 and the Wigner distributions in Sec.3. The different definitions of orbital angular momentum are discussed in Sec.4. Then in Sec.5, both analytical and numerical results in our model are discussed in detail. The correlation between the quark and proton spins and quark spin and OAM correlations are discussed in Sec.6. The results are also compared with other models. The GTMDs in this model are briefly discussed in Sec.7 and finally we conclude in Sec.8.

2 Light-front diquark model

In the diquark spectator model, one of the three valence quarks interacts with external photon and other two valence quarks are considered as a diquark state of spin-0(scalar diquark) or spin-1 (vector diquark). Therefore the proton state $|P\,;S\rangle$ can be treated as a two particle state in the Fock-state expansion. In this paper we consider the scalar diquark model developed in [17, 18]. The average light-front momentum of the scalar diquark is $P_X = \big((1-x)P^+, P_X^-, -\mathbf{p}_\perp\big)$, where x is the longitudinal momentum fraction carried by the struck quark.

The two-particle fock-state expansion for $J^z = \pm\frac{1}{2}$ are given by

$$|P;\pm\rangle = \sum_q \int \frac{dx\ d^2\mathbf{p}_\perp}{2(2\pi)^3\sqrt{x(1-x)}} \Big[\psi^{\pm}_{q+}(x,\mathbf{p}_\perp)|+\frac{1}{2},0;xP^+,\mathbf{p}_\perp\rangle + \psi^{\pm}_{q-}(x,\mathbf{p}_\perp)|-\frac{1}{2},0;xP^+,\mathbf{p}_\perp\rangle\Big], \quad (1)$$

Where the $|\lambda_q,\lambda_s;xP^+,\mathbf{p}_\perp\rangle$ represents a 2-particle state with a quark of helicity λ_q, and a diquark(spectator) of helicity λ_s. The xP^+ and $\mathbf{p}_\perp$ are the longitudinal momentum and transverse momentum of the active quark respectively. The $\psi^{\lambda_N}_{q\lambda_q}$ are the light-front wave functions corresponding to the nucleon helicity $\lambda_N = \pm$ and quark helicity $\lambda_q = \pm$. We adopt the generic ansatz for the quark-diquark model of the valence Fock state of the nucleon LFWFs [17], assuming vanishing quark mass

$$\begin{aligned}
\psi^{+}_{q+}(x,\mathbf{p}_\perp) &= \phi^{(1)}_q(x,\mathbf{p}_\perp),\\
\psi^{+}_{q-}(x,\mathbf{p}_\perp) &= -\frac{p^1+ip^2}{xM}\phi^{(2)}_q(x,\mathbf{p}_\perp),\\
\psi^{-}_{q+}(x,\mathbf{p}_\perp) &= \frac{p^1-ip^2}{xM}\phi^{(2)}_q(x,\mathbf{p}_\perp),\\
\psi^{-}_{q-}(x,\mathbf{p}_\perp) &= \phi^{(1)}_q(x,\mathbf{p}_\perp),
\end{aligned} \quad (2)$$

where $\varphi^{(1)}_q(x,\mathbf{p}_\perp)$ and $\varphi^{(2)}_q(x,\mathbf{p}_\perp)$ are the wave functions predicted by soft-wall AdS/QCD in [19] with the AdS/QCD scale parameter $\kappa = 0.4\ GeV$.

$$\varphi^{(i)}_q(x,\mathbf{p}_\perp) = N^{(i)}_q\frac{4\pi}{\kappa}\sqrt{\frac{\log(1/x)}{1-x}}x^{a^{(i)}_q}(1-x)^{b^{(i)}_q} \exp\Big[-\frac{\mathbf{p}_\perp^2}{2\kappa^2}\frac{\log(1/x)}{(1-x)^2}\Big], \quad (3)$$

The values of the parameters $a^{(i)}_q$, $b^{(i)}_q$ and $N^{(i)}_q$ are fixed in [20,21] by fitting the nucleon form-factor data. For completeness, we list the parameters in Table 1. This is a very simplistic model of the proton. It describes the proton by a scalar diquark and a quark and does not assume the $SU(4)$ symmetry of the usual diquark models where both scalar and axial vector diquarks are considered.

parameters	$a^{(1)}$	$a^{(2)}$	$b^{(1)}$	$b^{(2)}$	$N^{(1)}$	$N^{(2)}$
u quark	0.02	1.05	0.022	-0.15	2.055	1.322
d quark	0.1	1.07	0.38	-0.2	1.7618	-2.4827

Table 1 The parameters in the light front diquark model for $\kappa = 0.4$ GeV.

3 Wigner distribution

In the light-front framework, the 5-dimensional Wigner distribution is defined as [22] :

$$\rho^{q[\Gamma]}(\mathbf{b}_\perp,\mathbf{p}_\perp,x;S) = \int\frac{d^2\mathbf{\Delta}_\perp}{(2\pi)^2}e^{-i\mathbf{\Delta}_\perp.b_\perp}W^{q[\Gamma]}(\mathbf{\Delta}_\perp,\mathbf{p}_\perp,x;S) \quad (4)$$

Where the correlator $W^{[\Gamma]}$ at at $\Delta^+ = 0$ and fixed light-cone time $z^+ = 0$, is given by[10]:

$$W^{q[\Gamma]}(\mathbf{\Delta}_\perp,\mathbf{p}_\perp,x;S) = \frac{1}{2}\int\frac{dz^-}{(2\pi)}\frac{d^2z_T}{(2\pi)^2}e^{ip.z} \langle P'';S|\,\bar\psi^q(-z/2)\Gamma\mathcal{W}_{[-z/2,z/2]}\psi^q(z/2)|P';S\rangle\Big|_{z^+=0} \quad (5)$$

with the Dirac structure Γ e.g, $\gamma^+, \gamma^+\gamma^5$. The $P' = (P^+, P'^-, \frac{\mathbf{\Delta}_\perp}{2})$ and the $P'' = (P^+, P''^- - \frac{\mathbf{\Delta}_\perp}{2})$ are the initial and final momentum of proton. The $W^{[\Gamma]}$ depends on the average momentum $P = \frac{1}{2}(P'' + P')$ of proton, average quark momentum $\mathbf{p}_\perp = \frac{1}{2}(\mathbf{p}''_\perp + \mathbf{p}'_\perp)$, the proton helicity S and the transverse momentum transfer to the proton$\mathbf{\Delta}_\perp = (P''_\perp - P'_\perp)$. The Wilson line $\mathcal{W}_{[-z/2,z/2]}$ ensures the gauge invariance of the operator. We choose the symmetric frame where the components of 4-momentums, with skewness $\xi = 0$, are

$$P = [P^+, P^-, \mathbf{0}_\perp], \tag{6}$$

$$p = [xP^+, p^-, \mathbf{p}_\perp], \tag{7}$$

$$\Delta = [0, 0, \mathbf{\Delta}_\perp], \tag{8}$$

with $P^- = \frac{1}{2}(P''^- + P'^-) = \frac{4M^2 + \mathbf{\Delta}_\perp^2}{4P^+}$ (we use the notation $v^\pm = v^0 \pm v^3$). We calculate the matrix element of Eq.(5) in scalar diquark model using the wave functions predicted by soft-wall AdS/QCD. The Wigner distributions, with the proton helicity Λ and the quark helicity λ, for unpolarized and longitudinally polarized proton is defined as:

$$\rho^q_{\Lambda\lambda}(\mathbf{b}_\perp, \mathbf{p}_\perp, x) = \frac{1}{2}[\rho^{q[\gamma^+]}(\mathbf{b}_\perp, \mathbf{p}_\perp, x; \Lambda\hat{S}_z) + \lambda\rho^{q[\gamma^+\gamma^5]}(\mathbf{b}_\perp, \mathbf{p}_\perp, x; \Lambda\hat{S}_z)], \tag{9}$$

which can be decomposed as:

$$\rho^q_{\Lambda\lambda}(\mathbf{b}_\perp, \mathbf{p}_\perp, x) = \frac{1}{2}[\rho^q_{UU}(\mathbf{b}_\perp, \mathbf{p}_\perp, x) + \Lambda\rho^q_{LU}(\mathbf{b}_\perp, \mathbf{p}_\perp, x) + \lambda\rho^q_{UL}(\mathbf{b}_\perp, \mathbf{p}_\perp, x) + \Lambda\lambda\rho^q_{LL}(\mathbf{b}_\perp, \mathbf{p}_\perp, x)]. \tag{10}$$

corresponding to the proton spin $\Lambda = \uparrow, \downarrow$ and quark spin $\lambda = \uparrow, \downarrow$ (where $\uparrow$ and $\downarrow$ are corresponding to $+1$ and -1 respectively). Where the Wigner distribution $\rho^q_{UU}(\mathbf{b}_\perp, \mathbf{p}_\perp, x)$ of unpolarized quarks in an unpolarized proton, and the distortions $\rho^q_{LU}(\mathbf{b}_\perp, \mathbf{p}_\perp, x)$ due to unpolarized quarks in a longitudinally polarized proton, $\rho^q_{UL}(\mathbf{b}_\perp, \mathbf{p}_\perp, x)$ due to longitudinally polarized quarks in an unpolarized proton and $\rho^q_{LL}(\mathbf{b}_\perp, \mathbf{p}_\perp, x)$ due to longitudinally polarized quark in a longitudinally polarized proton, are defined as

$$\rho^q_{UU}(\mathbf{b}_\perp, \mathbf{p}_\perp, x) = \frac{1}{2}[\rho^{q[\gamma^+]}(\mathbf{b}_\perp, \mathbf{p}_\perp, x; +\hat{S}_z) + \rho^{q[\gamma^+]}(\mathbf{b}_\perp, \mathbf{p}_\perp, x; -\hat{S}_z)], \tag{11}$$

$$\rho^q_{LU}(\mathbf{b}_\perp, \mathbf{p}_\perp, x) = \frac{1}{2}[\rho^{q[\gamma^+]}(\mathbf{b}_\perp, \mathbf{p}_\perp, x; +\hat{S}_z) - \rho^{q[\gamma^+]}(\mathbf{b}_\perp, \mathbf{p}_\perp, x; -\hat{S}_z)], \tag{12}$$

$$\rho^q_{UL}(\mathbf{b}_\perp, \mathbf{p}_\perp, x) = \frac{1}{2}[\rho^{q[\gamma^+\gamma^5]}(\mathbf{b}_\perp, \mathbf{p}_\perp, x; +\hat{S}_z) + \rho^{q[\gamma^+\gamma^5]}(\mathbf{b}_\perp, \mathbf{p}_\perp, x; -\hat{S}_z)], \tag{13}$$

$$\rho^q_{LL}(\mathbf{b}_\perp, \mathbf{p}_\perp, x) = \frac{1}{2}[\rho^{q[\gamma^+\gamma^5]}(\mathbf{b}_\perp, \mathbf{p}_\perp, x; +\hat{S}_z) - \rho^{q[\gamma^+\gamma^5]}(\mathbf{b}_\perp, \mathbf{p}_\perp, x; -\hat{S}_z)]. \tag{14}$$

These four distributions are related with the Fourier transforms of the GTMDs as:

$$\rho^q_{UU}(\mathbf{b}_\perp, \mathbf{p}_\perp, x) = \mathcal{F}^q_{1,1}(x, 0, \mathbf{p}^2_\perp, \mathbf{p}_\perp.\mathbf{b}_\perp, \mathbf{b}^2_\perp), \tag{15}$$

$$\rho^q_{LU}(\mathbf{b}_\perp, \mathbf{p}_\perp, x) = -\frac{1}{M^2}\epsilon^{ij}_\perp p^i_\perp \frac{\partial}{\partial b^j_\perp}\mathcal{F}^q_{1,4}(x, 0, \mathbf{p}^2_\perp, \mathbf{p}_\perp.\mathbf{b}_\perp, \mathbf{b}^2_\perp), \tag{16}$$

$$\rho^q_{UL}(\mathbf{b}_\perp, \mathbf{p}_\perp, x) = \frac{1}{M^2}\epsilon^{ij}_\perp p^i_\perp \frac{\partial}{\partial b^j_\perp}\mathcal{G}^q_{1,1}(x, 0, \mathbf{p}^2_\perp, \mathbf{p}_\perp.\mathbf{b}_\perp, \mathbf{b}^2_\perp), \tag{17}$$

$$\rho^q_{LL}(\mathbf{b}_\perp, \mathbf{p}_\perp, x) = \mathcal{G}^q_{1,4}(x, 0, \mathbf{p}^2_\perp, \mathbf{p}_\perp.\mathbf{b}_\perp, \mathbf{b}^2_\perp). \tag{18}$$

Where the $\chi^q = \mathcal{F}^q_{1,1}, \mathcal{F}^q_{1,4}, \mathcal{G}^q_{1,1}, \mathcal{G}^q_{1,4}$ can be expressed as Fourier transform of corresponding GTMDs $X^q = F^q_{1,1}, F^q_{1,4}, G^q_{1,1}, G^q_{1,4}$.

$$\chi^q(x, 0, \mathbf{p}^2_\perp, \mathbf{p}_\perp.\mathbf{b}_\perp, \mathbf{b}^2_\perp) = \int \frac{d^2\mathbf{\Delta}_\perp}{(2\pi)^2} e^{-i\mathbf{\Delta}_\perp.\mathbf{b}_\perp} X^q(x, 0, \mathbf{p}^2_\perp, \mathbf{p}_\perp.\mathbf{\Delta}_\perp, \mathbf{\Delta}^2_\perp), \tag{19}$$

Integrating over all the variables, the Wigner distributions give

$$\int dx d^2\mathbf{p}_\perp d^2\mathbf{b}_\perp \rho^q_{UU}(\mathbf{b}_\perp, \mathbf{p}_\perp, x) = n_q, \tag{20}$$

$$\int dx d^2\mathbf{p}_\perp d^2\mathbf{b}_\perp \rho^q_{LU}(\mathbf{b}_\perp, \mathbf{p}_\perp, x) = 0, \tag{21}$$

$$\int dx d^2\mathbf{p}_\perp d^2\mathbf{b}_\perp \rho^q_{UL}(\mathbf{b}_\perp, \mathbf{p}_\perp, x) = 0, \tag{22}$$

$$\int dx d^2\mathbf{p}_\perp d^2\mathbf{b}_\perp \rho^q_{LL}(\mathbf{b}_\perp, \mathbf{p}_\perp, x) = \Delta q. \tag{23}$$

Where the n_q is the flavor factors, $n_u = 2$, $n_d = 1$ and the Δq is the axial charge.

Wigner distributions cannot have a direct probabilistic interpretation, however integrating over momentum and position, Wigner distributions can be reduced to probability distributions. Integrating over $\mathbf{b}_\perp$ with $\mathbf{\Delta}_\perp = 0$, the Wigner distributions reduce to the transverse momentum dependent parton distributions(TMDs). At $z_\perp = 0$, the $\mathbf{p}_\perp$ integration of Wigner distributions give generalized parton distributions(GPDs). The unpolarized TMD $f^q_1(x, \mathbf{p}^2_\perp)$ and GPD $H^q(x, 0, \mathbf{\Delta}^2_\perp)$ can be extracted as

$$f^q_1(x, \mathbf{p}^2_\perp) = F^q_{1,1}(x, 0, \mathbf{p}^2_\perp, 0, 0), \tag{24}$$

$$H^q(x, 0, \mathbf{\Delta}^2_\perp) = \int d^2\mathbf{p}_\perp F^q_{1,1}(x, 0, \mathbf{p}^2_\perp, \mathbf{p}_\perp.\mathbf{\Delta}_\perp, \mathbf{\Delta}^2_\perp) \tag{25}$$

and the TMD $g^q_{1L}(x, \mathbf{p}^2_\perp)$ and GPD $\tilde{H}^q(x, 0, \mathbf{\Delta}^2_\perp)$ can be expressed as:

$$g^q_{1L}(x, \mathbf{p}^2_\perp) = G^q_{1,4}(x, 0, \mathbf{p}^2_\perp, 0, 0), \tag{26}$$

$$\tilde{H}^q(x, 0, \mathbf{\Delta}^2_\perp) = \int d^2\mathbf{p}_\perp G^q_{1,4}(x, 0, \mathbf{p}^2_\perp, \mathbf{p}_\perp.\mathbf{\Delta}_\perp, \mathbf{\Delta}^2_\perp) \tag{27}$$

The $\mathbf{p}_\perp$ and $\mathbf{b}_\perp$ integration of the ρ^q_{LU} and ρ^q_{UL} give zero. So, there are no TMD and GPD corresponding to $F_{1,4}$ and $G_{1,1}$ GTMDs.

The Wigner distributions can also be reduced to three dimensional quark densities by integrating over two mutually orthogonal components of transverse position and momentum, e,g. b_y and p_x (b_x and p_y), which are not constraint by Heisenberg uncertainty principle as:

$$\int db_y dp_x \rho^{q[\Gamma]}(\mathbf{b}_\perp, \mathbf{p}_\perp, x; S) = \tilde{\rho}^{q[\Gamma]}(b_x, p_y, x; S), \quad (28)$$

with $\Delta_y = z_x = 0$. Note that the integration over other mixed transverse components b_x and p_y gives the same quark density as Eq.(28), with a opposite momentum i.e, $\tilde{\rho}^{q[\Gamma]}(b_y, p_x, x; S) = \tilde{\rho}^{q[\Gamma]}(b_x, -p_y, x; S)$. These relations are true only when there is axial symmtery i.e., for unpolarized or longitudinally polarized proton.

4 Orbital angular momentum

Jaffe and Manohar showed in the light-cone gauge that the spin of the nucleon can be decomposed into the quark spin, quark OAM, gluon spin and gluon OAM[23].

$$S^q + \ell^q + S^g + \ell^g = \frac{1}{2}. \quad (29)$$

For the diquark model, the above sum rule can be written as

$$S^q + \ell^q + S^D + \ell^D = \frac{1}{2}, \quad (30)$$

where the super-script D is for diquark, and for scalar diquark $S^D = 0$. The canonical OAM operator for quark is defined as

$$\hat{\ell}^q_z(b^-, \mathbf{b}_\perp, p^+, \mathbf{p}_\perp) = \frac{1}{2}\int \frac{dz^- d^2\mathbf{z}_\perp}{(2\pi)^3} e^{ip.z}$$
$$\bar{\psi}^q(b^- - \frac{z^-}{2}, \mathbf{b}_\perp)\gamma^+ \quad (\mathbf{b}_\perp \times (-i \overleftrightarrow{\partial}_\perp))\psi^q(b^- + \frac{z^-}{2}, \mathbf{b}_\perp). \quad (31)$$

From the definition of Wigner operator (Eq.(5)), the OAM density operator can be expressed as

$$\hat{\ell}^q_z = 2(\mathbf{b}_\perp \times \mathbf{p}_\perp)\hat{W}^{q[\gamma^+]}. \quad (32)$$

Thus in light-front gauge the average canonical OAM for quark is written in terms of Wigner distribution as.

$$\ell^q_z = \int \frac{d\Delta^+ d^2\mathbf{\Delta}_\perp}{2P^+(2\pi)^3}\langle P''; S|\hat{\ell}^q_z|P'; S\rangle$$
$$= \int dx d^2\mathbf{p}_\perp d^2\mathbf{b}_\perp (\mathbf{b}_\perp \times \mathbf{p}_\perp)_z \rho^{q[\gamma^+]}(\mathbf{b}_\perp, \mathbf{p}_\perp, x, \hat{S}_z) \quad (33)$$

Where, the distribution $\rho^{q[\gamma^+]}(\mathbf{b}_\perp, \mathbf{p}_\perp, x, \hat{S}_z)$ can be written from Eqs.(11,12) as:

$$\rho^{q[\gamma^+]}(\mathbf{b}_\perp, \mathbf{p}_\perp, x, +\hat{S}_z) = \rho^q_{UU}(\mathbf{b}_\perp, \mathbf{p}_\perp, x) + \rho^q_{LU}(\mathbf{b}_\perp, \mathbf{p}_\perp, x) \quad (34)$$

From Eq.(15) we see that

$$\int dx d^2\mathbf{p}_\perp d^2\mathbf{b}_\perp (\mathbf{b}_\perp \times \mathbf{p}_\perp)_z \rho^q_{UU}(\mathbf{b}_\perp, \mathbf{p}_\perp, x) = 0, \quad (35)$$

which satisfies the angular momentum sum rule for unpolarized proton, the total angular momentum of constituents sum up to zero. Using Eq.(16) and Eq.(19), the twist-2 canonical quark OAM in the light-front gauge is

$$\ell^q_z = -\int dx d^2\mathbf{p}_\perp \frac{\mathbf{p}^2_\perp}{M^2} F^q_{1,4}(x, 0, \mathbf{p}^2_\perp, 0, 0). \quad (36)$$

The Jaffe-Manohar decomposition (Eq.(29)) is not gauge invariant. Ji proposed a gauge invariant decomposition of nucleon spin as[24]

$$S^q + L^q + J^g = \frac{1}{2}, \quad (37)$$

where L^q is the kinetic OAM for the quark q. However, Chen et al.[25] proposed an idea to decompose the gauge field A_μ into a pure gauge part, A^{pure}_μ, and a physical part, A^{phy}_μ to give a gauge invariant definition of the Jaffe-Manohar decomposition.

The kinetic OAM of quark appearing in the Ji sum rule is defined in terms of GPDs as[24]:

$$L^q_z = \frac{1}{2}\int dx \left[x\Big(H^q(x,0,0) + E^q(x,0,0)\Big) - \tilde{H}^q(x,0,0)\right] \quad (38)$$

where $H^q(x,\xi,t)$ and $E^q(x,\xi,t)$ are unpolarized GPDs and $\tilde{H}^q(x,\xi,t)$ is the helicity dependent GPD. In our model calculation, the explicit expressions are given in Sec.5. A comparative study between longitudinal component of canonical OAM and kinetic OAM are shown in the Fig. 1 and the values are given in Table 2. Note that the above relation (Eq.38) does not hold for density level interpretation in the transverse plane [26].

The spin-orbit correlation is given by the operator

$$C^q_z(b^-, \mathbf{b}_\perp, p^+, \mathbf{p}_\perp) = \frac{1}{2}\int \frac{dz^- d^2\mathbf{z}_\perp}{(2\pi)^3} e^{ip.z}$$
$$\bar{\psi}^q(b^- - \frac{z^-}{2}, \mathbf{b}_\perp)\,\gamma^+\gamma^5(\mathbf{b}_\perp \times (-i \overleftrightarrow{\partial}_\perp))\psi^q(b^- + \frac{z^-}{2}, \mathbf{b}_\perp). \quad (39)$$

The correlation between quark spin and quark OAM can be expressed with Wigner distributions ρ^q_{UL} and equivalently in terms of GTMD as:

$$C^q_z = \int dx d^2\mathbf{p}_\perp d^2\mathbf{b}_\perp (\mathbf{b}_\perp \times \mathbf{p}_\perp)_z \rho^q_{UL}(\mathbf{b}_\perp, \mathbf{p}_\perp, x)$$
$$= \int dx d^2\mathbf{p}_\perp \frac{\mathbf{p}^2_\perp}{M^2} G^q_{1,1}(x, 0, \mathbf{p}^2_\perp, 0, 0). \quad (40)$$

Where $C^q_z > 0$ implies the quark spin and OAM tend to be aligned and $C^q_z < 0$ implies they are anti-aligned. In our model, the quark spin and OAM tend to be anti-aligned for both u and d quarks.

One can see from Eq.(18), a similar correlator with ρ^q_{LL} vanishes

$$\int dx d^2\mathbf{p}_\perp d^2\mathbf{b}_\perp (\mathbf{b}_\perp \times \mathbf{p}_\perp)_z \rho^q_{LL}(\mathbf{b}_\perp, \mathbf{p}_\perp, x) = 0. \quad (41)$$

5 Results

We calculate the Wigner distributions of proton in light-front AdS/QCD quark-diquark model. Using Eq.(1) in Eq.(5) the quark-quark correlator, $W^{q[\Gamma]}(\mathbf{\Delta}_\perp, \mathbf{p}_\perp, x; S)$, can be expressed in terms of LFWFs as.

$$W^{q[\gamma^+]}(\mathbf{\Delta}_\perp, \mathbf{p}_\perp, x; \pm\hat{S}_z) = \frac{1}{16\pi^3}\Big[\psi^{\pm\dagger}_{q+}(x, \mathbf{p}''_\perp)\psi^{\pm}_{q+}(x, \mathbf{p}'_\perp) + \psi^{\pm\dagger}_{q-}(x, \mathbf{p}''_\perp)\psi^{\pm}_{q-}(x, \mathbf{p}'_\perp)\Big], \quad (42)$$

$$W^{q[\gamma^+\gamma^5]}(\mathbf{\Delta}_\perp, \mathbf{p}_\perp, x; \pm\hat{S}_z) = \frac{1}{16\pi^3}\Big[\psi^{\pm\dagger}_{q+}(x, \mathbf{p}''_\perp)\psi^{\pm}_{q+}(x, \mathbf{p}'_\perp) - \psi^{\pm\dagger}_{q-}(x, \mathbf{p}''_\perp)\psi^{\pm}_{q-}(x, \mathbf{p}'_\perp)\Big]. \quad (43)$$

for the Dirac structures $\Gamma = \gamma^+, \gamma^+\gamma^5$. In the symmetric frame the initial and final momentums of the struck quark are

$$\mathbf{p}'_\perp = \mathbf{p}_\perp - (1-x)\frac{\mathbf{\Delta}_\perp}{2}, \quad (44)$$

$$\mathbf{p}''_\perp = \mathbf{p}_\perp + (1-x)\frac{\mathbf{\Delta}_\perp}{2} \quad (45)$$

respectively. Using the wave functions from Eq.(2,3) in Eqs.(42,43), the explicit expressions for Wigner distributions are

$$\rho^q_{UU}(\mathbf{b}_\perp, \mathbf{p}_\perp, x) = \frac{1}{16\pi^3}\int \frac{d\Delta_\perp}{2\pi}\Delta_\perp \mathrm{J}_0(|\Delta_\perp||\mathrm{b}_\perp|) \exp\big(-2\tilde{a}(x)\tilde{\mathbf{p}}^2_\perp\big)\Big[|A^{(1)}_q(x)|^2 + \Big(\mathbf{p}^2_\perp - \frac{\mathbf{\Delta}^2_\perp}{4}(1-x)^2\Big)\frac{1}{M^2x^2}|A^{(2)}_q(x)|^2\Big], \quad (46)$$

$$\rho^q_{LU}(\mathbf{b}_\perp, \mathbf{p}_\perp, x) = -\frac{1}{M^2}\epsilon^{ij}_\perp p^i_\perp \frac{\partial}{\partial b^j_\perp}\Big[-\frac{1}{16\pi^3}\int\frac{d\Delta_\perp}{2\pi} \Delta_\perp \mathrm{J}_0(|\Delta_\perp||\mathrm{b}_\perp|)\exp\big(-2\tilde{a}(x)\tilde{\mathbf{p}}^2_\perp\big)\frac{(1-x)}{x^2}|A^{(2)}_q(x)|^2\Big], \quad (47)$$

$$\rho^q_{UL}(\mathbf{b}_\perp, \mathbf{p}_\perp, x) = \frac{1}{M^2}\epsilon^{ij}_\perp p^i_\perp \frac{\partial}{\partial b^j_\perp}\Big[-\frac{1}{16\pi^3}\int\frac{d\Delta_\perp}{2\pi} \Delta_\perp \mathrm{J}_0(|\Delta_\perp||\mathrm{b}_\perp|)\exp\big(-2\tilde{a}(x)\tilde{\mathbf{p}}^2_\perp\big)\frac{(1-x)}{x^2}|A^{(2)}_q(x)|^2\Big], \quad (48)$$

$$\rho^q_{LL}(\mathbf{b}_\perp, \mathbf{p}_\perp, x) = \frac{1}{16\pi^3}\int \frac{d\Delta_\perp}{2\pi}\Delta_\perp \mathrm{J}_0(|\Delta_\perp||\mathrm{b}_\perp|) \exp\big(-2\tilde{a}(x)\tilde{\mathbf{p}}^2_\perp\big)\Big[|A^{(1)}_q(x)|^2 - \Big(\mathbf{p}^2_\perp - \frac{\mathbf{\Delta}^2_\perp}{4}(1-x)^2\Big)\frac{1}{M^2x^2}|A^{(2)}_q(x)|^2\Big], \quad (49)$$

Where

$$A^{(i)}_q(x) = N^{(i)}_q \frac{4\pi}{\kappa}\sqrt{\frac{\log(1/x)}{(1-x)}}x^{a^{(i)}_q}(1-x)^{b^{(i)}_q}, \quad (50)$$

$$\tilde{a}(x) = \frac{\log(1/x)}{2\kappa^2(1-x)^2}, \quad (51)$$

$$\tilde{\mathbf{p}}^2_\perp = \mathbf{p}^2_\perp + \frac{\mathbf{\Delta}^2_\perp}{4}(1-x)^2. \quad (52)$$

At the limit $\xi = 0$, the GTMDs are

$$F^q_{1,1}(x, \mathbf{\Delta}^2_\perp, \mathbf{p}^2_\perp) = \frac{1}{16\pi^3}\Big[|A^{(1)}_q(x)|^2 + \Big(\mathbf{p}^2_\perp - \frac{\mathbf{\Delta}^2_\perp}{4}(1-x)^2\Big)\frac{1}{M^2x^2}|A^{(2)}_q(x)|^2\Big]\exp\big[-2\tilde{a}(x)\tilde{\mathbf{p}}^2_\perp\big], \quad (53)$$

$$F^q_{1,4}(x, \mathbf{\Delta}_\perp, \mathbf{p}^2_\perp) = -\frac{1}{16\pi^3}\Big[\frac{(1-x)}{x^2}|A^{(2)}_q(x)|^2\Big]\exp\big[-2\tilde{a}(x)\tilde{\mathbf{p}}^2_\perp\big], \quad (54)$$

$$G^q_{1,1}(x, \mathbf{\Delta}^2_\perp, \mathbf{p}^2_\perp) = -\frac{1}{16\pi^3}\Big[\frac{(1-x)}{x^2}|A^{(2)}_q(x)|^2\Big]\exp\big[-2\tilde{a}(x)\tilde{\mathbf{p}}^2_\perp\big], \quad (55)$$

$$G^q_{1,4}(x, \mathbf{\Delta}_\perp, \mathbf{p}^2_\perp) = \frac{1}{16\pi^3}\Big[|A^{(1)}_q(x)|^2 - \Big(\mathbf{p}^2_\perp - \frac{\mathbf{\Delta}^2_\perp}{4}(1-x)^2\Big)\frac{1}{M^2x^2}|A^{(2)}_q(x)|^2\Big]\exp\big[-2\tilde{a}(x)\tilde{\mathbf{p}}^2_\perp\big]. \quad (56)$$

We find $F^q_{1,4} = G^q_{1,1}$ to the leading order as found in [27] for scalar diquark model. Thus the distributions $\rho^q_{LU} = -\rho^q_{UL}$.

From Eq.(36), the canonical OAM can be written as

$$\ell^q_z = \int dx \ell^q_z(x). \quad (57)$$

Using Eq.(54), $\ell^q_z(x)$ can be written as

$$\ell^q_z(x) = \frac{\kappa^2}{M^2\log(1/x)}F^q_2(x)(1-x)^5. \quad (58)$$

In this model, ℓ^q_z can also be related with pretzelosity $h^\perp_{1T}$ as

$$\ell^q_z = -\int dx d^2\mathbf{p}_\perp \frac{\mathbf{p}^2_\perp}{2M^2}(1-x)h^{q\perp}_{1T}(x, \mathbf{p}^2_\perp). \quad (59)$$

$h^{q\perp}_{1T}(x, \mathbf{p}^2_\perp)$ is one of the eight leading twist TMDs. In this light-front scalar diquark model $h^{q\perp}_{1T}(x, \mathbf{p}^2_\perp)$ is written as[21]

$$h^{q\perp}_{1T}(x, \mathbf{p}^2_\perp) = -\frac{2\log(1/x)}{\pi\kappa^2}\exp\Big[-\frac{\mathbf{p}^2_\perp\log(1/x)}{\kappa^2(1-x)^2}\Big]F^q_2(x) \quad (60)$$

where $F^q_2(x)$ is given in Eq(67). Using Eq.(53) and Eq.(56) in Eq.(25) and (27), the GPDs H and $\tilde{H}$ can be ex-

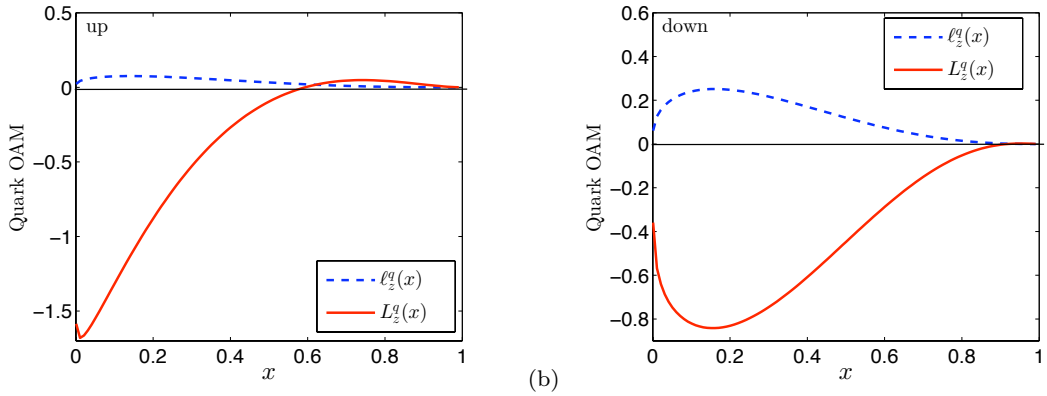

(a) (b)

Fig. 1 The variation of canonical OAM $\ell_z^q(x)$ and kinetic OAM $L_z^q(x)$ with longitudinal momentum fraction x, for (a) u quark and (b) d quark.

pressed as

$$H^q(x,0,t) = \Big[F_1^q(x)(1-x)^2 + F_2^q(x)(1-x)^4\frac{\kappa^2}{M^2\log(1/x)}\Big] (1-\frac{|t|}{4\kappa^2}\log(1/x))\exp\Big[-\frac{|t|}{4\kappa^2}\log(1/x)\Big], \quad (61)$$

$$\tilde{H}^q(x,0,t) = \Big[F_1^q(x)(1-x)^2 - F_2^q(x)(1-x)^4\frac{\kappa^2}{M^2\log(1/x)}\Big] (1+\frac{|t|}{4\kappa^2}\log(1/x))\exp\Big[-\frac{|t|}{4\kappa^2}\log(1/x)\Big]. \quad (62)$$

In the AdS/QCD light-front scalar diquark model the helicity flip GPD E is given[18] as

$$E^q(x,0,t) = 2F_3^q(x)(1-x)^3\exp\Big[-\frac{|t|}{4\kappa^2}\log(1/x)\Big] \quad (63)$$

Where $Q^2 = -q^2 = -t$, the square of the momentum transferred in the process and is taken to be zero for OAM calculation.

The kinetic OAM of quarks(Eq.(38)) can be written as

$$L_z^q = \int dx L_z^q(x). \quad (64)$$

Where in this model, using Eqs.(61), (62) and Eq.(63) at $t=0$ limit, the $L_z^q(x)$ reads

$$L_z^q(x) = \frac{1}{2}\Big[-F_1^q(x)(1-x)^3 + F_2^q(x)(1-x)^4(1+x) \frac{\kappa^2}{M^2\log(1/x)} + 2F_3^q(x)x(1-x)^3\Big]. \quad (65)$$

Where

$$F_1^q(x) = |N_q^{(1)}|^2 x^{2a_q^{(1)}}(1-x)^{2b_q^{(1)}-1}, \quad (66)$$

$$F_2^q(x) = |N_q^{(2)}|^2 x^{2a_q^{(2)}-2}(1-x)^{2b_q^{(2)}-1}, \quad (67)$$

$$F_3^q(x) = N_q^{(1)}N_q^{(2)} x^{a^{(1)}+a_q^{(2)}-1}(1-x)^{b_q^{(1)}+b_q^{(2)}-1}. \quad (68)$$

The variation of the quark OAMs $\ell_z^q(x)$ and $L_z^q(x)$ with longitudinal momentum fraction x is sown in Fig.1 for u and d quark.

5.1 Unpolarized proton

In our numerical study, we have considered the active quark to be either a u or d quark, the spectator always being a diquark. In other words, when we calculate the Wigner distribution for the u quark, we have not incorporated any contribution from the u quark that is part of the diquark. The first Mellin moment of $\rho_{UU}^q(\mathbf{b}_\perp, \mathbf{p}_\perp, x)$ is shown in Fig.2. Fig.2(a) and Fig.2(b) represent the distributions in transverse momentum plane for u quark and d quark respectively. The fixed impact parameter $\mathbf{b}_\perp$ is taken along $\hat{y}$ and $b_y = 0.4\ fm$. The variation of $\rho_{UU}^q(\mathbf{b}_\perp, \mathbf{p}_\perp)$ in the transverse impact parameter plane are shown in Fig.2(c) and Fig.2(d) for u and d quark respectively, with fixed transverse momentum $\mathbf{p}_\perp$ along $\hat{y}$ for $p_y = 0.3\ GeV$. The distributions ρ_{UU}^u and ρ_{UU}^d are circularly symmetric, in transverse momentum plane as well as transverse impact parameter plane, with a positive maxima at the centre $(p_x = p_y = 0)$, $(b_x = b_y = 0)$ and gradually decrease towards periphery, for both u and d quarks. The peak of the distribution for u quark is large compare to d quark in both the planes.

The average quadrupole distortions $Q_b^{ij}(\mathbf{p}_\perp)$ and $Q_p^{ij}(\mathbf{b}_\perp)$ are defined as[10]

$$Q_b^{ij}(\mathbf{p}_\perp) = \frac{\int d^2\mathbf{b}_\perp(2b_\perp^i b_\perp^j - \delta^{ij}\mathbf{b}_\perp^2)\rho_{UU}(\mathbf{b}_\perp, \mathbf{p}_\perp)}{\int d^2\mathbf{b}_\perp \mathbf{b}_\perp^2 \rho_{UU}(\mathbf{b}_\perp, \mathbf{p}_\perp)} \quad (69)$$

$$Q_p^{ij}(\mathbf{b}_\perp) = \frac{\int d^2\mathbf{p}_\perp(2p_\perp^i p_\perp^j - \delta^{ij}\mathbf{p}_\perp^2)\rho_{UU}(\mathbf{b}_\perp, \mathbf{p}_\perp)}{\int d^2\mathbf{p}_\perp \mathbf{p}_\perp^2 \rho_{UU}(\mathbf{b}_\perp, \mathbf{p}_\perp)}. \quad (70)$$

In this model, the average quadrupole distortion is found to be zero. Since the wave functions in soft-wall AdS/QCD model are of gaussian type, the ρ_{UU} and ρ_{LL} are even in $\mathbf{p}_\perp$ and $\mathbf{b}_\perp$ resulting to the zero quadrupole distortion.

As we discussed before, the three dimensional quark densities can be extracted from the Wigner distributions by integrating over one transverse momentum p_x

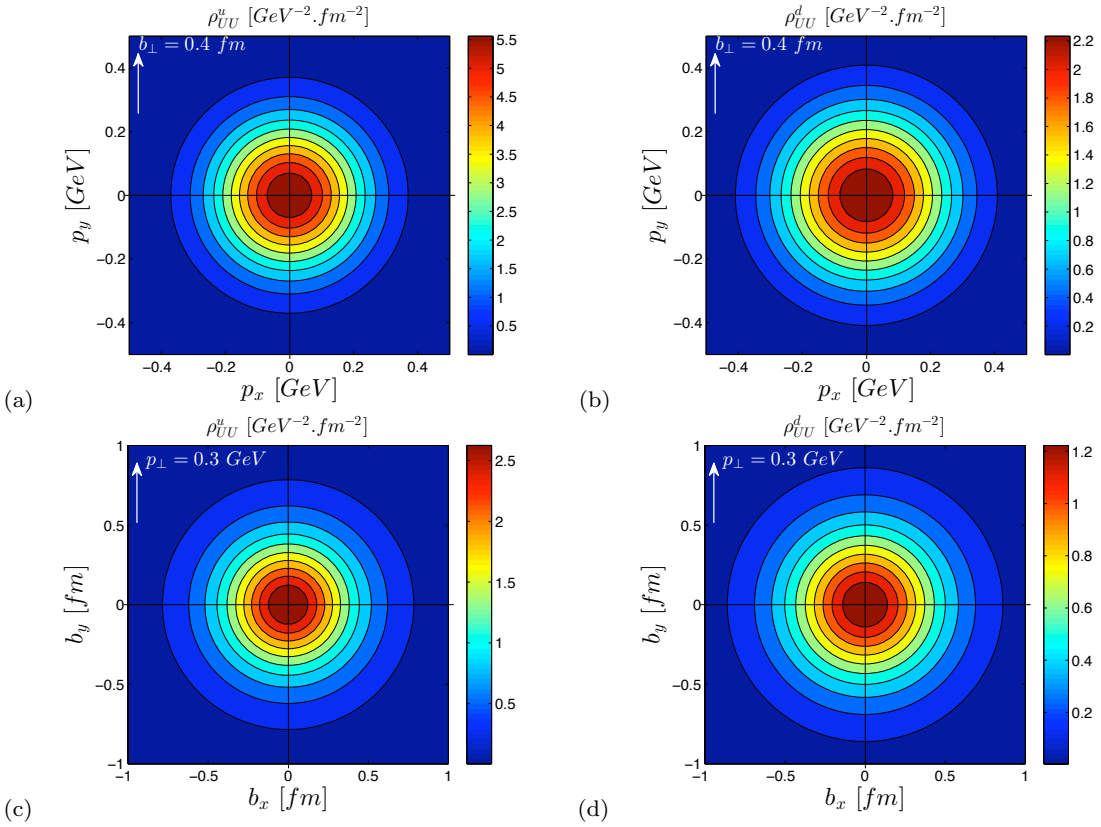

Fig. 2 The Wigner distributions of unpolarized quarks in an unpolarized proton in the transverse momentum plane(a,b) with $\mathbf{b}_\perp = 0.4\hat{y}\ fm$ and in the transverse impact parameter plane(c,d) with $\mathbf{p}_\perp = 0.3\hat{y}\ GeV$ for u quarks(left column) and d quarks(right column).

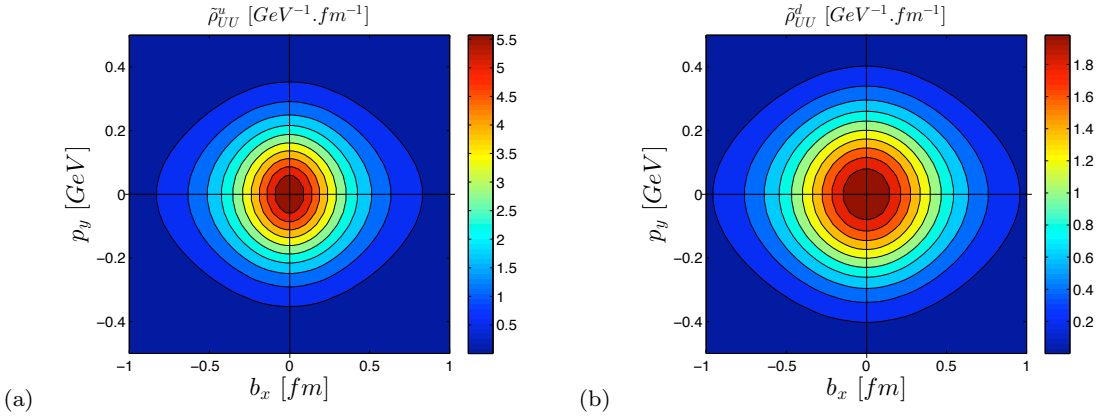

Fig. 3 $\tilde{\rho}^q_{UU}(b_x, p_y)$ in mixed transverse plane for u quark(a) and d quark(b).

and one transverse position b_y variables(see Eq.(28)). $\tilde{\rho}_{UU}(b_x, p_y)$ in mixed transverse plane are shown in Fig.3 for u and d quarks. We find that the distributions are axially symmetric. Therefore, there is no favored configuration between $\mathbf{b}_\perp \perp \mathbf{p}_\perp$ and $\mathbf{b}_\perp \parallel \mathbf{p}_\perp$ unlike the light-cone constituent quark model(LCCQM) [11] or chiral quark soliton model(χQSM) [13]. At $b_x = p_y = 0$, the probability density for u and d quark is maximum and decreases as $e^{-\alpha p_y^2}$ and $e^{-\beta b_x^2}$. Where the α and β are positive constants and we observe $\alpha > \beta$ for both u and d quarks .

The Wigner distributions $\rho^q_{UL}(\mathbf{b}_\perp, \mathbf{p}_\perp)$, in the transverse momentum plane, are shown in Fig.4(a) and (b) for u and d quarks respectively. The fixed transverse impact parameter $\mathbf{b}_\perp$ is along $\hat{y}$ with $b_y = 0.4\ fm$. The Fig.4(c) and (d) represent the distribution $\rho^q_{UL}(\mathbf{b}_\perp, \mathbf{p}_\perp)$ in transverse impact parameter plane, for u and d quark for $\mathbf{p}_\perp = p_y\hat{y} = 0.3\ GeV$. We observe a dipolar dis-

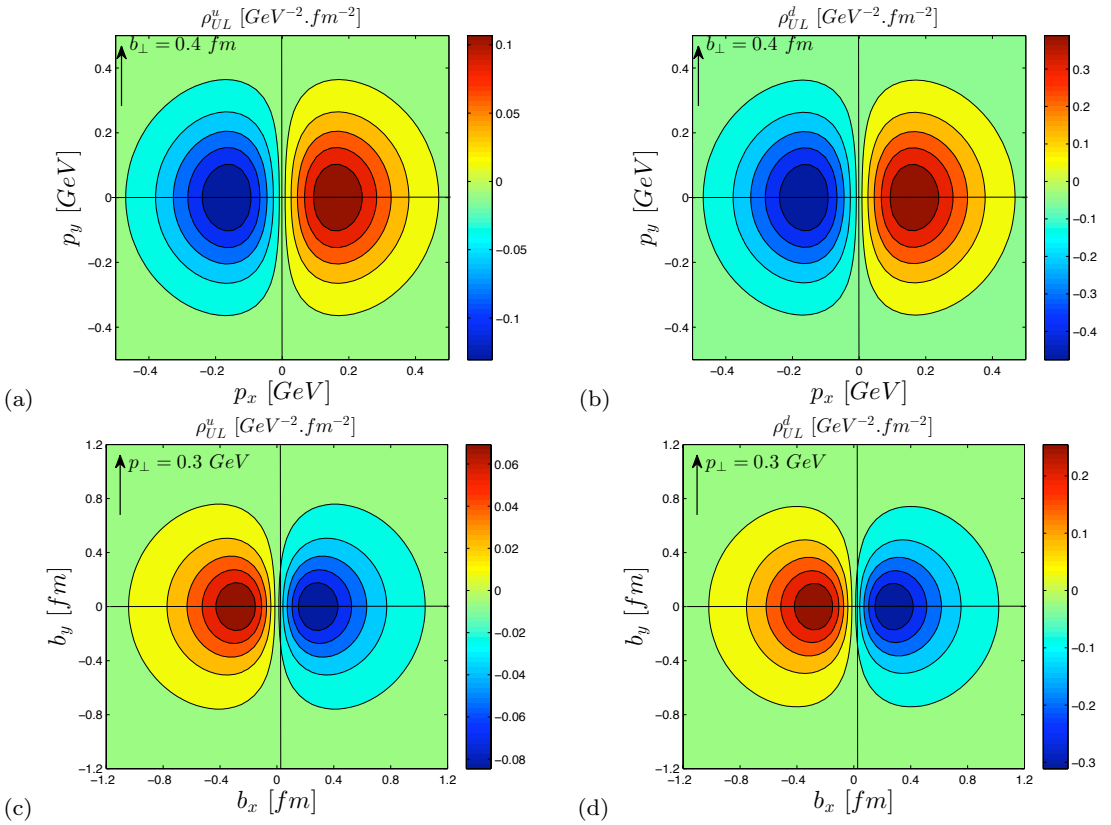

Fig. 4 The dipolar behavior of ρ^q_{UL} in the transverse momentum plane(a,b) with $\mathbf{b}_\perp = 0.4\hat{y}\ fm$ and in the transverse impact parameter plane(c,d) with $\mathbf{p}_\perp = 0.3\hat{y}\ GeV$ for u quarks(left column) and d quarks(right column).

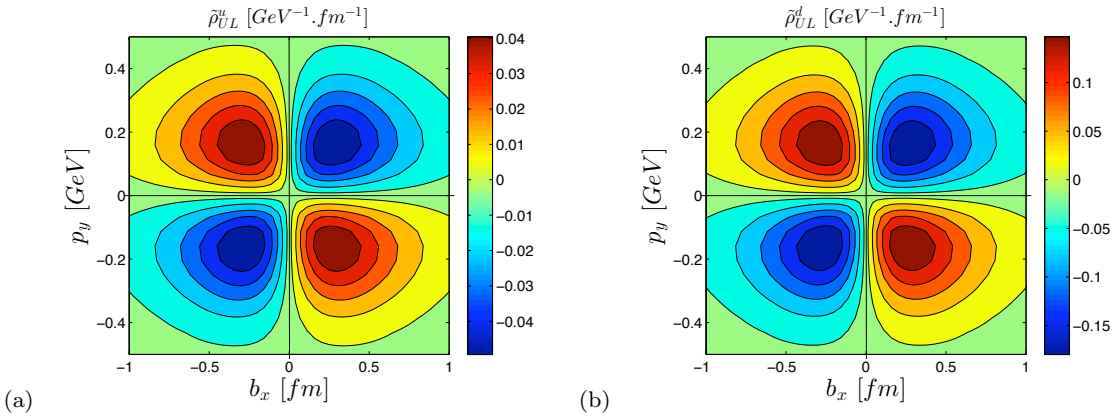

Fig. 5 $\tilde{\rho}^q_{UL}(b_x, p_y)$ in mixed transverse plane corresponding to u quark(a) and d quark(b).

tributions having same polarity for u and d quarks. $\tilde{\rho}^q_{UL}(b_x, p_y)$ in the transverse mixed plane are shown in Fig.5. We find a quadrupole distribution for u and d quarks. Using Eq.(55) in Eq.(40) we calculate the C^q_z, the correlation between quark spin and quark OAM. The values are: $C^u_z = -0.0348$ for u quark and $C^d_z = -0.1201$ for d quarks. Therefore in this model, the quark OAM tends to be anti-aligned($C^u_z < 0, C^d_z < 0$) to quark spin for both u and d quarks.

5.2 Longitudinally Polarized Proton

The Wigner distributions $\rho^q_{LU}(\mathbf{b}_\perp, \mathbf{p}_\perp)$ are shown in Fig.6 for u and d quarks. Fig.6(a) and (b) show the variation of $\rho^q_{LU}(\mathbf{b}_\perp, \mathbf{p}_\perp)$ in transverse momentum plane for u and d quarks respectively with $\mathbf{b}_\perp$ is along $\hat{y}$ and $b_y = 0.4\ fm$. The variation of $\rho^q_{LU}(\mathbf{b}_\perp, \mathbf{p}_\perp)$ in transverse impact parameter plane is shown in Fig.6(c) and (d) with fixed $\mathbf{p}_\perp$ along $\hat{y}$, $p_y = 0.3\ GeV$. We find dipolar distributions for u and d quarks. The polarity of the

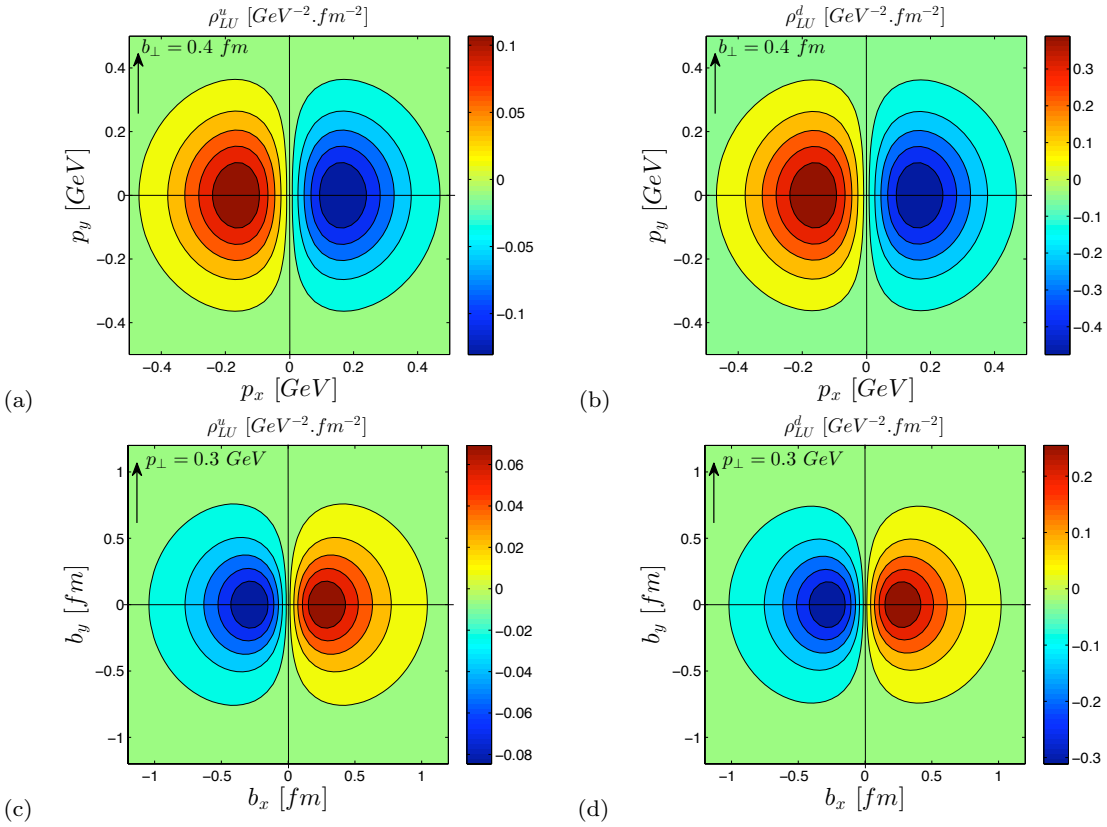

Fig. 6 The dipolar behavior of ρ^q_{LU} in the transverse momentum plane(a,b) with $\mathbf{b}_\perp = 0.4\hat{y}\ fm$ and in the transverse impact parameter plane(c,d) with $\mathbf{p}_\perp = 0.3\hat{y}\ GeV$ for u quarks(left column) and d quarks(right column).

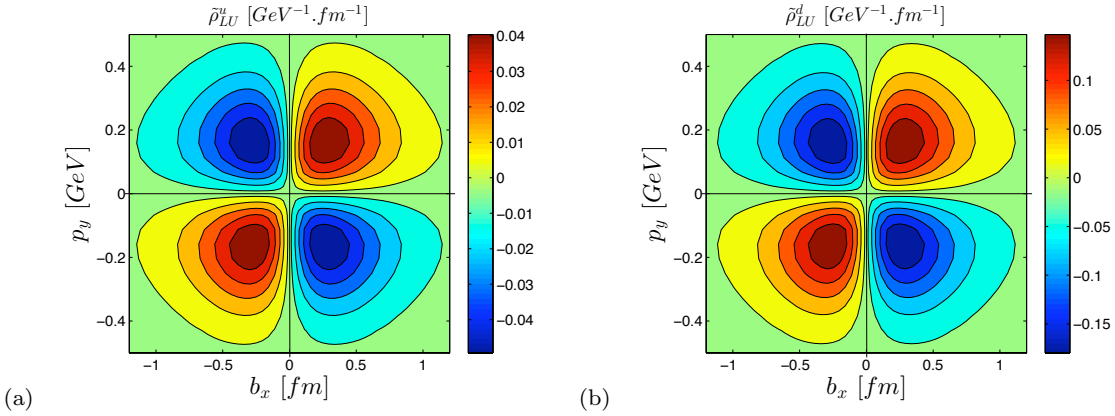

Fig. 7 The $\tilde{\rho}^q_{LU}(b_x, p_y)$ in mixed transverse plane corresponding to u quark(a) and d quark(b).

dipolar distribution ρ^q_{LU} is opposite to the polarity of ρ^q_{UL} . The maximum value of $\rho^q_{LU}(\mathbf{b}_\perp, \mathbf{p}_\perp)$ for u quark is less than that for d quarks in both the planes. Fig.7(a) and (b) represent the distribution $\tilde{\rho}^q_{LU}(b_x, p_y)$ in the mixed transverse plane for u and d quarks respectively. We observe quadrupole distributions for both u and d quarks. The quadrupole structures in $\rho^q_{LU}(\mathbf{b}_\perp, \mathbf{p}_\perp)$ and $\rho^q_{UL}(\mathbf{b}_\perp, \mathbf{p}_\perp)$ are found due to the presence of the derivative terms in Eq.(16) and Eq.(17).

	q-OAM	u	d
Canonical	ℓ^q_z	0.0348	0.1201
Kinetic	L^q_z	-0.3812	-0.4258

Table 2 In the light-front AdS/QCD scalar diquark model, the values of canonical OAM ℓ^q_z and the kinetic OAM L^q_z for u and d quark.

From Eqs.(57) and (64), we calculate the canonical OAM and kinetic OAM of quarks in this model. The values of quark OAM are given in Table.2. Note that

in quark-diquark model, the total proton OAM is given by the sum of quark and diquark angular momenta, so unlike the quark models u and d quark contributions do not add upto the total proton OAM and hence the sum of kinetic OAM of u and d in Table.2 is not the same as total canonical OAM of the u and d. The correlation between the canonical OAM of quark and proton spin can be understood from the sign of the ℓ_z^q. In our model calculation, the positive values of ℓ_z^q for both u and d imply that the proton spin tends to be aligned to quark OAM for both u and d quarks. The spin contribution of the quark to the proton spin is given by[10]

$$s^q = \frac{1}{2}\Delta q = \frac{1}{2}\int dx \tilde{H}^q(x,0,0) = \frac{1}{2}\int dx\ d^2p_\perp G^q_{1,4}(x,0,\mathbf{p}_\perp^2,0,0) \qquad (71)$$

where Δq is the axial charge. In our model, we get $s^u = 0.946$ and $s^d = 0.396$. It is well known that the spectator diquark model has its own limitations[28]. Though the functional behaviors of the GPDs and GTMDs are well reproduced in our model, the axial charges for both u and d quarks are over estimated. The model is defined at a very low scale $Q_0^2 \approx 0.09\ GeV^2$. The axial charge is scale dependent and known to be negative at larger scales. In [17], the authors have extended the result to an arbitrary scale Q^2 and studied the evolution of unpolarized pdfs in this model. Our result agrees closely with theirs, in spite of the fact that the fit parameters are slightly different. In their model [29], the pdfs are slightly smaller in magnitude. When polarized pdfs or helicity distributions are computed, the d quark helicity distribution comes out to be positive, although it is expected to be negative from the recent fit of the data [30]. In [31], it has been shown that NNPDF allows for a positive total $\Delta d(x)/d(x)$ (where $\Delta d(x)$ stands for helicity distribution)for larger values of x, this is also obtained in some other models, for example in [32], the above ratio was calculated in perturbative QCD taking into account the valence Fock components with non-vanishing orbital angular momentum and it was found that $\Delta d(x)/d(x)$ is positive as $x \approx 0.75$ and approaches 1 as $x \to 1$. Positive values of this ratio was also found in an SU(6) breaking quark model calculation in [33]. Another way to parametrize the model would be to fit the data of the helicity distributions with the model parameters, instead of the form factors and the GPDs. Since in the scalar diquark model, $\ell_z^q + s^q + \ell_z^D = 1/2$ (as $s^D = 0$), the diquark contribution to the canonical OAM is $\ell_z^D = -0.484$ for u struck-quark and $\ell_z = -0.016$ for d struck-quark. The contributions of different partial waves to the quark OAM in LCCQM have been studied in [12].

The Wigner distributions for longitudinally polarized quark in a longitudinally polarized proton, $\rho^q_{LL}(\mathbf{b}_\perp, \mathbf{p}_\perp)$, are shown in Fig.8. The Fig.8(a) and (b) represent $\rho^q_{LL}(\mathbf{b}_\perp, \mathbf{p}_\perp)$ in transverse momentum plane with fixed $\mathbf{b}_\perp = 0.4\ fm\ \hat{y}$ and Fig.8(c) and (d) show the plots in the transverse impact parameter plane with $\mathbf{p}_\perp = 0.3\ GeV\ \hat{y}$. The distributions are circularly symmetric for u and d quarks in both the planes. The circular symmetry implies that the ρ_{LL} can not contribute to the quark OAM as shown in Eq.(41). The picks of the distributions are at the centre (0,0) in both the planes. Therefore the quark polarization and the proton polarization tend to be parallel for u and d quarks. Fig.9 represents the distribution $\tilde{\rho}^q_{LL}(b_x, p_y)$ in a mixed transverse plane. The distributions are axially symmetric for both u and d quarks.

The distributions $\rho^q_{\Lambda\lambda}(\mathbf{b}_\perp, \mathbf{p}_\perp)$ are shown in Fig.10 and Fig.11 with the polarization of proton $\Lambda = \uparrow$ and quark polarization $\lambda = \uparrow, \downarrow$(Eq.(10)). Figs.10(a-d) represent the variation of $\rho^q_{\Lambda\lambda}(\mathbf{b}_\perp, \mathbf{p}_\perp)$ in the transverse momentum plane for u and d quarks. We observe a circular symmetry for $\Lambda = \lambda$ but for $\Lambda \neq \lambda$ the distributions get distorted along p_x for both u and d quarks. This is because, in Eq(9), the contributions from ρ_{LU} and $\rho_{UL} (\rho_{LU} = -\rho_{UL})$ get cancelled for $\Lambda = \lambda$, whereas for $\Lambda \neq \lambda$, the contributions add up and causes the distortion. We have shown the distributions for $\Lambda = \uparrow$, the other possible spin combinations in transverse momentum plane can be found from $\rho^q_{\downarrow\lambda'}(\mathbf{b}_\perp, p_x, p_y) = \rho^q_{\uparrow\lambda}(\mathbf{b}_\perp, -p_x, p_y)$, where $\lambda' \neq \lambda$. Figs.10(e-h) show the variation of $\rho^q_{\Lambda\lambda}(\mathbf{b}_\perp, \mathbf{p}_\perp)$ in transverse impact parameter plane for u and d quarks. The distributions are circularly symmetric in transverse impact parameter space for $\Lambda = \lambda$ but the distributions get distorted for $\Lambda \neq \lambda$, due to the same reason as described in case of transverse momentum plane. Similar to the momentum space, the other possible spin combinations in the transverse impact parameter plane are found as $\rho^q_{\downarrow\lambda'}(b_x, b_y, \mathbf{p}_\perp) = \rho^q_{\uparrow\lambda}(-b_x, b_y, \mathbf{p}_\perp)$, where $\lambda' \neq \lambda$. The mixed transverse densities $\tilde{\rho}^q_{\Lambda\lambda}(b_x, p_y)$ are shown in Fig.11 for u and d quarks. Again, for $\Lambda = \lambda$ the contribution from quadrupole distortions (Fig.(5,7)) $\tilde{\rho}_{UL}$ and $\tilde{\rho}_{LU}$ get cancelled resulting the axial symmetry but for $\Lambda \neq \lambda$ the contributions add up. The maxima of $\tilde{\rho}_{UU}$ and $\tilde{\rho}_{LL}$ are nearly equal (Figs. 3 and 9). As a result, for $\Lambda \neq \lambda$, the destructive interference of these two distributions give almost zero at the centre$(b_x = 0, p_y = 0)$ in Fig.11(c,d).

6 Spin-Spin and Spin-OAM Correlation

In Fig. 4 and Fig. 6, we observe that the quark OAM tends to be anti-aligned with quark spin and aligned to the proton spin for both u and d quarks. The correlation

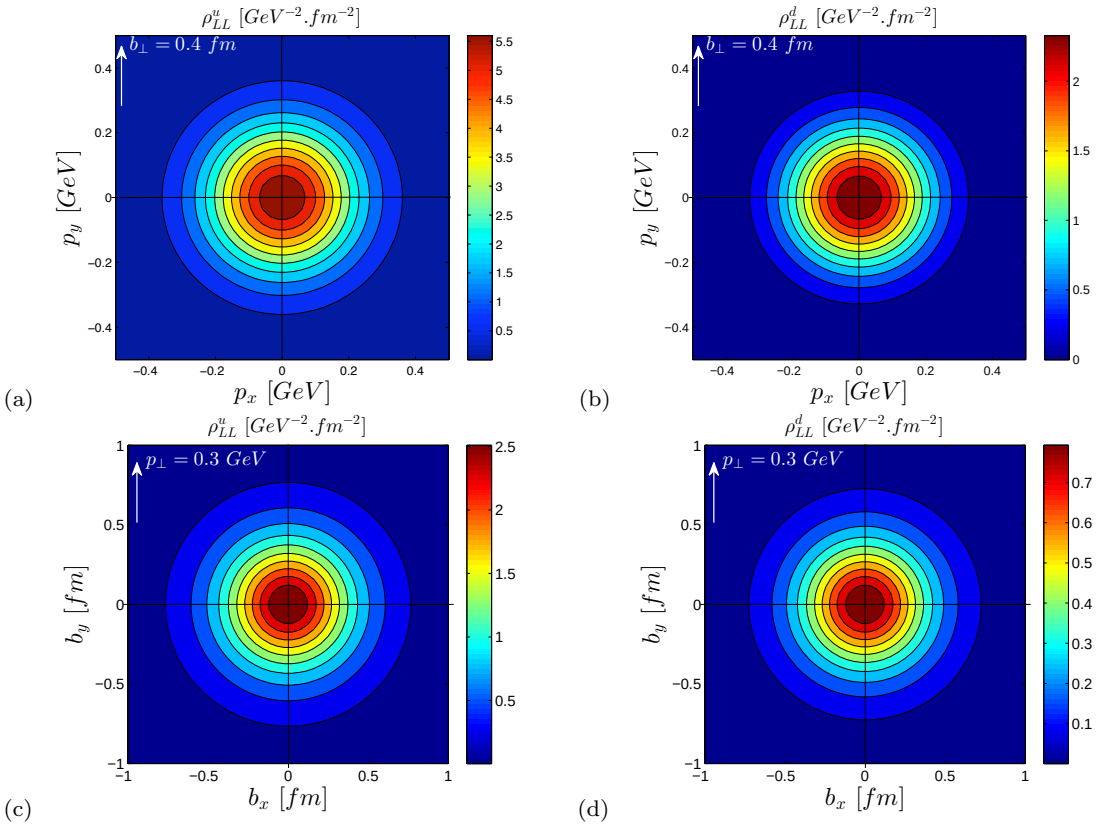

Fig. 8 The $\rho^q_{LL}(\mathbf{b}_\perp, \mathbf{p}_\perp)$ in the transverse momentum plane (a,b) with $\mathbf{b}_\perp = 0.4\hat{y}\ fm$ and in the transverse impact parameter plane(c,d) with $\mathbf{p}_\perp = 0.3\hat{y}\ GeV$ for u and d quarks respectively.

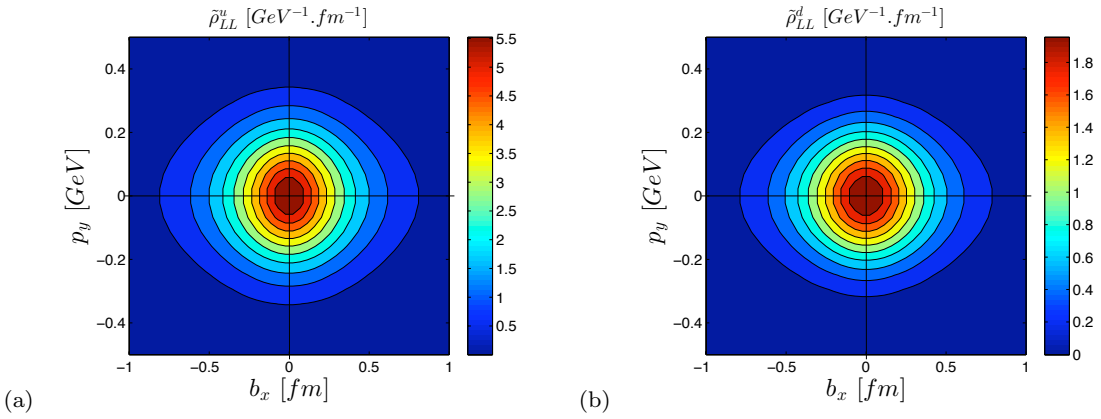

Fig. 9 The $\tilde{\rho}^q_{LL}(b_x, p_y)$ in mixed transverse plane for u and d quarks.

strength between proton spin and quark OAM is equal to the correlation between quark spin and quark OAM. Therefore, if the quark spin is parallel to the proton spin, i,e. $\Lambda = \uparrow, \lambda = \uparrow$ the contributions of ρ_{UL} and ρ_{LU} interfere destructively resulting the circular symmetry for u and d quarks, see Fig 10(a,b,e,f). If the quark spin is anti-parallel to the proton spin, i,e. $\Lambda = \uparrow, \lambda = \downarrow$ the contributions of ρ_{UL} and ρ_{LU} interfere constructively resulting a significant shift for u and d quarks, see Fig 10(c,d,g,h). One can notice that from Fig.10, the direction of shift flips with the polarization flip when $\Lambda \neq \lambda$.

We compare our results with the light cone constituent quark model (LCCQM) [10] and light cone spectator model [16] in the tables 3 and 4. The polarities of ρ_{UL} distributions are opposite to LCCQM but similar to the spectator model, whereas for ρ_{LU}, all the three models agree for u quark, but the agreement is lost for d-quark. In our model, the average quadrupole distortion $Q^{ij}_b(\mathbf{p}_\perp)$ and $Q^{ij}_p(\mathbf{b}_\perp)$, in both the trans-

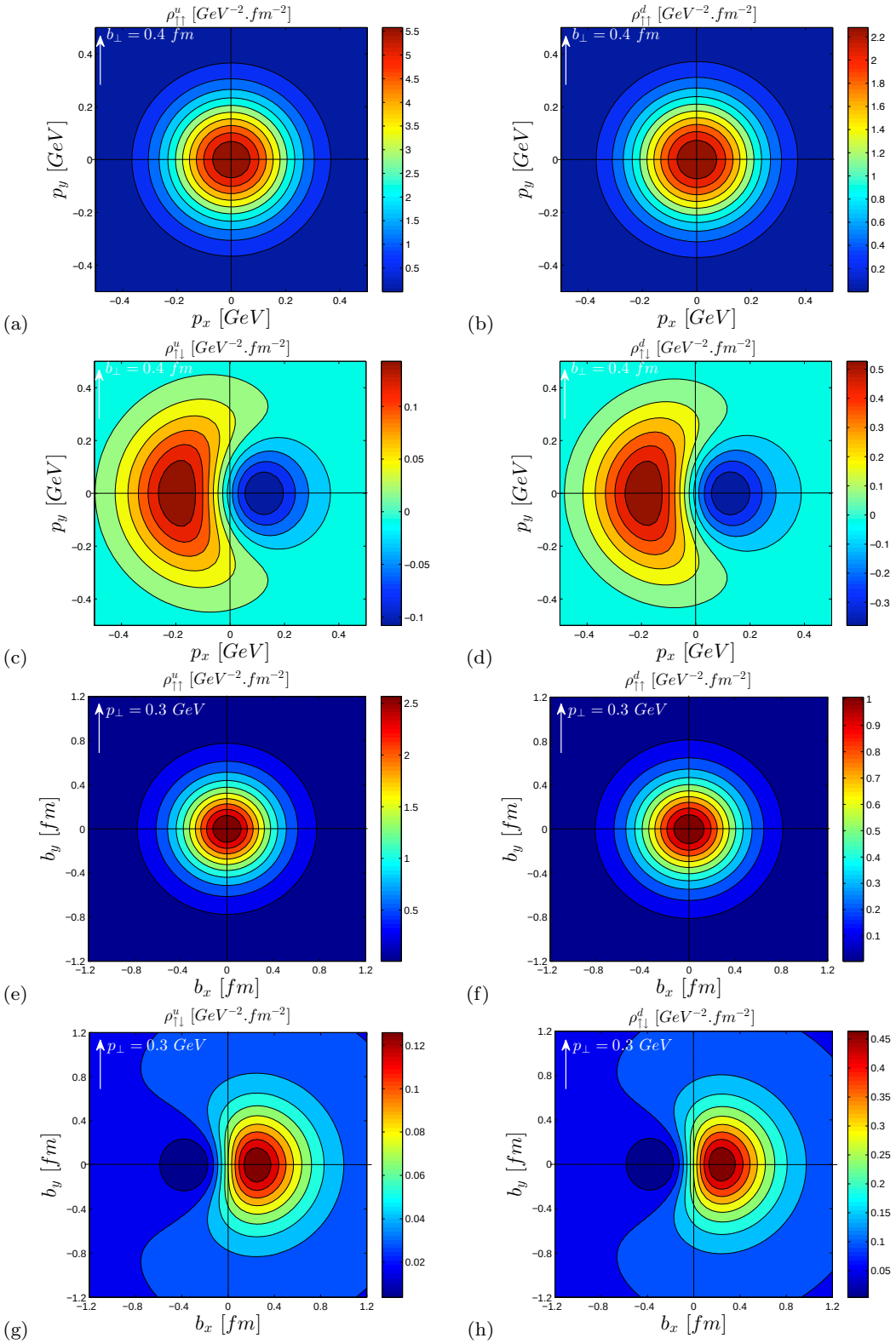

Fig. 10 The $\rho^q_{\Lambda\lambda}(\mathbf{b}_\perp, \mathbf{p}_\perp)$ for $\Lambda = \uparrow$ and $\lambda = \uparrow, \downarrow$ in transverse momentum plane(a-d)with $\mathbf{b}_\perp = 0.4\hat{y}\ fm$ and in transverse impact parameter plane(e-h)with $\mathbf{p}_\perp = 0.3\hat{y}\ GeV$ for u and d quarks.

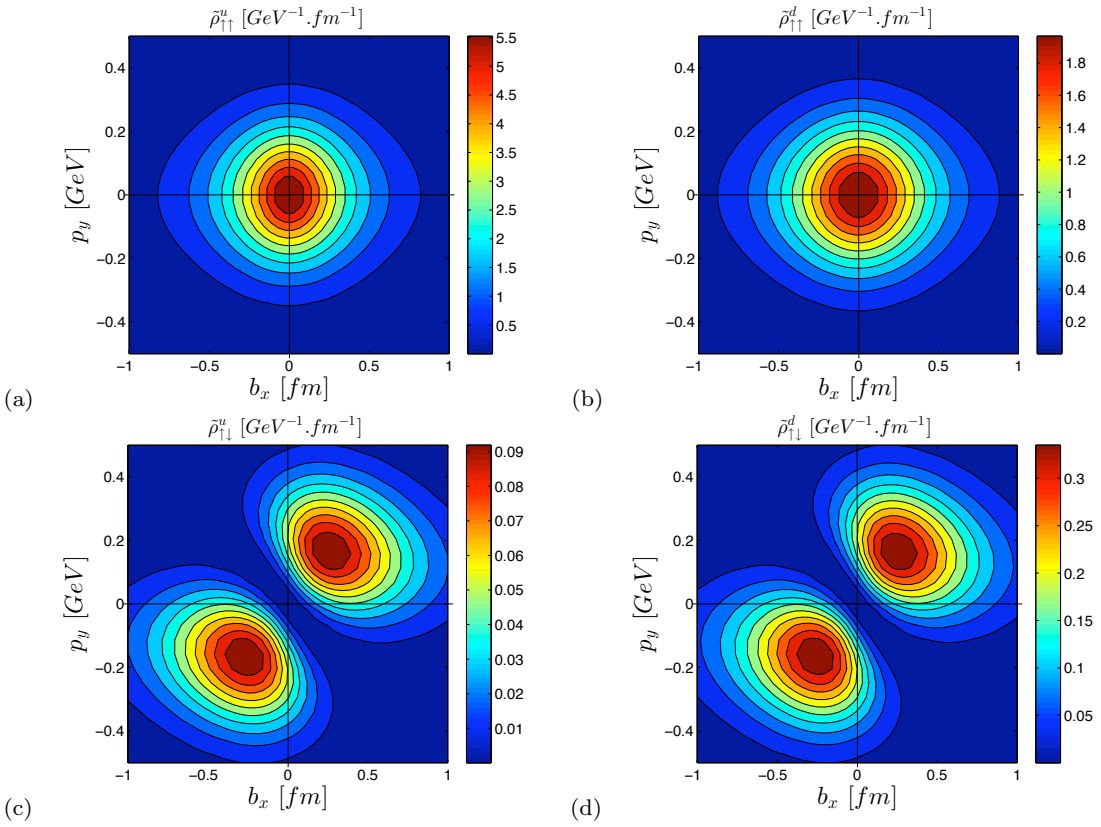

Fig. 11 The $\tilde{\rho}^{q}_{\Lambda\lambda}(b_x, p_y)$ for $\Lambda = \uparrow$ and $\lambda = \uparrow, \downarrow$ in mixed transverse plane for u and d quarks.

$\rho_{UL}(\mathbf{p}_\perp)$	Our Model	Ref.[10]	Ref.[16]	$\rho_{UL}(\mathbf{b}_\perp)$	Our Model	Ref.[10]	Ref.[16]
u	- + (0.1)	+ - (0.6)	- + (0.010)	u	+ - (0.06)	- + (0.5)	+ - (0.010)
d	- + (0.3)	‘ + - (0.6)	- + (0.005)	d	+ - (0.2)	- + (0.5)	+ - (0.005)

Table 3 Comparison of ρ_{UL} in different models in momentum space(left panel) and in impact parameter space(right panel). + -/- + represent the polarity of the dipolar distributions and the maxima of the distributions are given within the bracket.

$\rho_{LU}(\mathbf{p}_\perp)$	Our Model	Ref.[10]	Ref.[16]	$\rho_{LU}(\mathbf{b}_\perp)$	Our Model	Ref.[10]	Ref.[16]
u	+ - (0.1)	+ - (0.35)	+ - (0.010)	u	- + (0.06)	- + (0.3)	- + (0.005)
d	+ - (0.3)	- + (0.03)	- + (0.002)	d	- + (0.2)	+ - (0.015)	+ - (0.0005)

Table 4 Comparison of ρ_{LU} in different models in momentum space(left panel) and in impact parameter space(right panel). + -/- + represent the polarity of the dipolar distributions and the maxima of the distributions are given within the bracket.

verse momentum plane and transverse impact parameter plane, are found to be zero, whereas a nonzero small quadrupole distortion is found in [10]. This may be due the simple scalar diquark model considered here, inclusion of axial vector diquark might improve the result. The quark OAM tends to be anti-aligned($C^u_z < 0, C^d_z < 0$) to quark spin for both u and d quarks in our model, in LCCQM the quark OAM and quark spin tend to be aligned for both u and d quarks($C^u_z > 0,\ C^d_z > 0$). In our model, the quark OAM tends to be aligned to proton spin for both u and d quarks($\ell^u_z > 0,\ \ell^d_z > 0$). Whereas in [10], the quark OAM tends to be aligned($\ell^u_z > 0$) to proton spin for u quark and anti-aligned($\ell^d_z < 0$) for d quark. For proton spin anti-aligned with quark spin, the distributions $\rho^q_{\uparrow\downarrow}$ for both u and d quarks show stronger dipolar structure in our model compared to the LCCQM. QCD or some model independent calculations are required to resolve the differences.

7 GTMDs

At leading twist, there are sixteen GMDs. The variation of GTMDs (Eqs.(53-56)) for u and d quarks are shown in Fig.(12). The left column is for different values of $\Delta^2_\perp$ with a fixed $\mathbf{p}_\perp = 0.3\ GeV$ and the right column is for different values of $p_\perp$ with a fixed $\mathbf{\Delta}^2_\perp = 1.0\ GeV^2$. We observe that the peak of the distributions decrease with

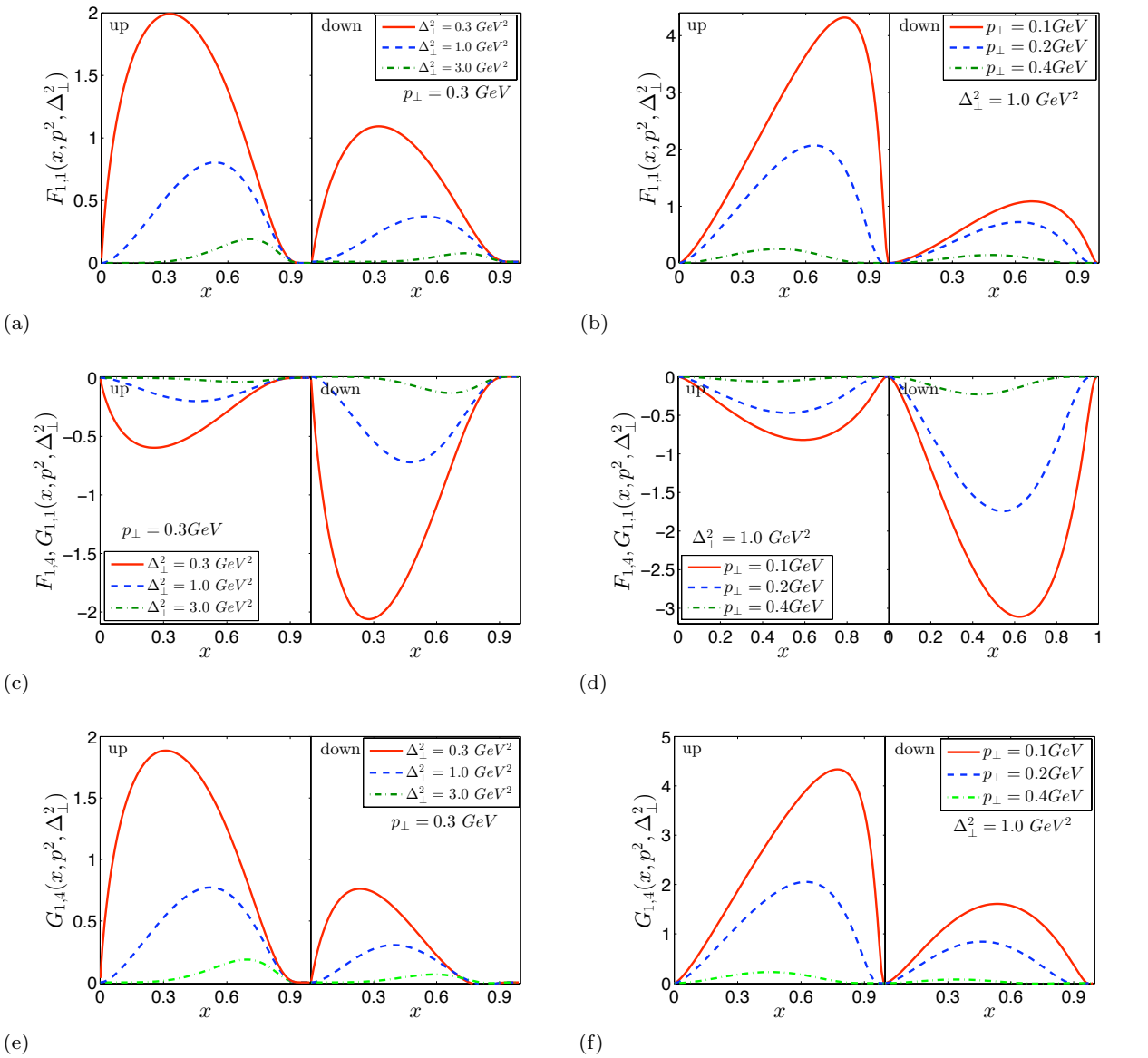

Fig. 12 GTMDs as functions of x for both u and d quarks at different fixed values of $\mathbf{p}_\perp$ and $\mathbf{\Delta}_\perp$.

increasing $\mathbf{\Delta}_\perp$ and shift towards higher x . Thus, the distributions $F^q_{1,1}, F^q_{1,4}, G^q_{1,1}, G^q_{1,4}$, having a quark with fixed transverse $\mathbf{p}_\perp$, highly depends on the momentum transfer $\mathbf{\Delta}_\perp$ between initial and final proton. The behavior of $F_{1,1}$ for u and d quarks are almost same except in magnitude which is larger for u quark than d quark. In $F_{1,4}(= G_{1,1})$, the maxima for d quark is greater than the maxima for u quark and opposite to $F_{1,1}$ and $G_{1,4}$. The GTMDs as functions of x are shown in the right column of Fig.12 for the different values of $\mathbf{p}_\perp$ with a fixed value of $\Delta_\perp^2 = 1.0\ GeV^2$. In this case, the peak of the distributions shift towards lower x and decreases as $\mathbf{p}_\perp$ increases.

8 conclusions

We have calculated the Wigner distributions in a quark-scalar diquark model of the proton. We have used the light-front wave functions for the state that are predicted by the soft wall ADS/QCD. The Wigner distributions of both unpolarized quark in unpolarized proton as well as the distortions in momentum and position space due to the polarization of the quark/proton are calculated. The results are compared and contrasted with other model estimates, in particular with those models that assume a confining potential. Wigner functions are related to GTMDs that give information on the canonical OAM as well as the spin-orbit correla-

tion of the quarks. The kinetic OAM can be calculated in terms of the GPDs in this model. We have calculated both the canonical and kinetic OAM and compared with other model calculations. In our case the proton state consists of an active quark which can be either a u or a d quark, and a scalar diquark. So the sum of the OAM of the u and and the d quark is not expected to be the same. In fact the kinetic and canonical OAM of the u quark are positive in this model whereas that of the d quark are negative. We have also calculated the pretzelosity in this model using a model-dependent relation. As $x \to 1$ the difference between kinetic and canonical OAM vanishes as all the momentum is carried by the active quark. Further work would involve calculation of Wigner distributions incorporating transverse polarization.

References

1. X. Ji, Phys. Rev. D. **55**, 7114 (1997).
2. A. V. Radyushkin, Phys. Rev. D **56**, 5524 (1997).
3. K. Goeke, M. V. Polyakov, M. Vanderhagen, Prog. Part. Nucl. Phys. **47**, 401 (2001).
4. M. Diehl, Phys. Rept **388**, 41 (2003).
5. J. C. Collins and D. E. Soper, Nucl. Phys. B **193**, 381 (1981).
6. D. Sivers, Phys. Rev. D **41**, 83 (1990).
7. P. J. Mulders and R. D. Tangerman, Nucl. Phys. B **461**, 197 (1996).
8. D. Boer and P. J. Mulders, Phys. Rev. D **57**, 5780 (1998).
9. X. Ji, Phys. Rev. Lett. **91**, 062001 (2003); A.V. Belitsky, X. Ji, and F. Yuan, Phys. Rev. D **69**, 074014 (2004).
10. C. Lorce and B. Pasquini, Phys. Rev. D **84**, 014015 (2011).
11. S. Boffi, B. Pasquini, and M. Traini, Nucl. Phys. B **649**, 243 (2003); B **680**, 147 (2004); B. Pasquini, M. Pincetti, and S. Boffi, Phys. Rev. D **72**, 094029 (2005); **76**, 034020 (2007); B. Pasquini, S. Cazzaniga, and S. Boffi, Phys. Rev. D **78**, 034025 (2008).
12. C. Lorce, B. Pasquini, X. Xiong, F. Yuan, Phys. Rv. D **85**, 114004 (2012).
13. C. Lorce, Phys. Rev. D **74**, 054019 (2006); C. Lorce, Phys. Rev. D **78**, 034001 (2008); C. Lorce, Phys. Rev. D **79**, 074027 (2009).
14. V. Y. Petrov and M. V. Polyakov, arXiv:hep-ph/0307077; D. Diakonov and V. Petrov, Phys. Rev. D **72**, 074009 (2005).
15. A. Mukherjee, S. Nair and V. K. Ojha, Phys. Rev. D **90**, no. 1, 014024 (2014); A. Mukherjee, S. Nair and V. K. Ojha, Phys. Rev. D **91**, no. 5, 054018 (2015).
16. Tianbo Liu and Bo-Qiang Ma, Phys. Rev. D **91**, 034019 (2015).
17. T. Gutsche, V. E. Lyubovitskij, I. Schmidt, A. Vega, Phy. Rev. D **89**, 054033 (2014).
18. C. Mondal, D. Chakrabarti, Eur. Phys. J. C **75**, 261 (2015).
19. S. J. Brodsky and G. F. de Téramond, arXiv:1203.4025 [hep-ph].
20. D. Chakrabarti and C. Mondal, Phys. Rev. D **92**, 074012 (2015).
21. T. Maji, C. Mondal, D. Chakrabarti and O. V. Teryaev, JHEP **1601**, 165 (2016).
22. S. Meissner, A. Metz, M. Schlegel, and K. Goeke, JHEP **0808**, 038 (2008); S. Meissner, A. Metz, and M. Schlegel, JHEP **0908**, 056 (2009).
23. R. I. Jaffe, A. Manohar, Nucl. Phys. B **337**, 509 (1990).
24. X. D. Ji, Phys. Rev. Lett. **78**, 610 (1997).
25. X. S. Chen, X. F. Lu, W. M. Sun, F. Wang and T. Goldman, Phys. Rev. Lett. **100**, 232002 (2008).
26. K. F. Liu and C. Lorc, Eur. Phys. J. A **52**, no. 6, 160 (2016).
27. K. Kanazawa, C. Lorce, A. Metz, B. Pasquini, M. Schlegel, Phy. Rev. D **90**, 014028(2014).
28. A. Becchetta, F. Conti and M. Radici, Phys. Rev. D **78**, 074010 (2008).
29. T. Gutsche, V. E. Lyubovitskij, I. Schmidt and A. Vega, Phys. Rev. D **91**, 054028 (2015).
30. D. de Florian, R. Sassot, M. Stratmann and W. Vogelsang, Phys. Rev. D **80**, 034030 (2009).
31. E. R. Nocera *et al* (NNPDF collaboration), Nucl. Phy. B **887**, 276 (2014); E. R. Nocera, Phys. Lett. B **742**, 117 (2015).
32. H. Avakian, S. J. Brodsky, A. Deur and F. Yuan, Phys. Rev. Lett. **99**, 082001 (2007).
33. F. Close, W. Melnitchouk, Phys. Rev. C **68**, 035210 (2003).